BLOCK AND INACTIVATION OF SODIUM CHANNELS IN NERVE BY AMINO ACID DERIVATIVES

II. Dependence on Temperature and Drug Concentration

Mei-Ven C. Lo and Peter Shrager, *Department of Physiology, University of Rochester Medical Center, Rochester, New York 14642*

ABSTRACT The interaction of *n*-propylguanidinium (*n*PG) with sodium channels has been further characterized. From experiments at varying temperatures, the Q_{10} for the sodium current decay time constant in the two [Na^+] gradients is 2.6–2.9 independent of drug. Testing several *n*PG concentrations we find that peak sodium current declines sharply with [*n*PG] at all levels, but the decay time constant approaches an asymptote above 4 mM. No "hooks" in sodium tail currents are seen. If the sodium current is allowed to decay completely before repolarization no tail current is observed. We have developed a kinetic model in which *n*PG acts at a single site within the sodium channel. Reaction of *n*PG with its receptor requires two steps. Fitting the temperature data shows that the first step involves diffusion of the drug to the site and close association with it. The second step may include molecular reorganization of the complex. The rate constants for the reaction are all simple exponential functions of voltage. Using them, the model successfully predicts decay time constants and peak currents, and their dependence on potential, [Na^+] gradient, temperature, and *n*PG concentration. The results are consistent with the idea that an arginine residue may be closely associated with inactivation.

INTRODUCTION

In the previous paper (Lo and Shrager, 1981) we examined *n*-propylguanidinium (*n*PG), the side chain of the amino acid arginine, for its ability to interact with the sodium channel in the axon membrane. We were especially interested in testing the idea that a peptide with a cationic amino acid might function as an endogenous blocking particle in the inactivation of normal sodium channels (Armstrong and Bezanilla, 1977; Rojas and Rudy, 1976; Yeh and Narahashi, 1977; Eaton et al., 1978; Cahalan and Almers, 1979*a*,*b*). *n*PG perfused internally resulted in a block of peak sodium conductance and a speeding of I_{Na} decay kinetics. Both of these effects were stronger at higher depolarizations and in axons in which the Na^+ concentration gradient was reversed. The results suggested that *n*PG acted within the sodium channel and pointed to a double mode of action, possibly at two distinct sites. In order to further resolve the mechanism involved we now report results of experiments at different temperatures and drug concentrations, and give records of sodium tail currents. A rather simple kinetic model requiring just one site is then proposed, as an aid in interpreting the results.

METHODS

Methods are identical to those of the previous paper (Lo and Shrager, 1981). Crayfish giant axons were internally perfused and were voltage clamped by an axial wire technique. Experimental pulse protocols

and ionic current analyses were run by a PDP8 computer. In "normal" $[Na^+]$ gradient, $[Na^+]_o$ = 211.7 mM and $[Na^+]_i$ = 15 mM. In "reversed" $[Na^+]$ gradient, $[Na^+]_o$ = 2.3 mM and $[Na^+]_i$ = 213 or 235 mM. Compositions of all external and internal solutions used are listed in Table I of Lo and Shrager (1981).

RESULTS

Temperature Dependence

As one means of characterizing the mechanism of action of *n*PG on sodium channels we have examined sodium currents of fibers at different temperatures. In Fig. 1 we show the dependence of I_{Na} decay time constant on temperature, drawn as an Arrhenius plot. The symbols represent experimental data at +90 mV, a potential at which effects of *n*PG are large. The straight lines are least-squares fits. Fig. 1 *A* is from an axon in normal $[Na^+]$ gradient and Fig. 1 *B* illustrates results in reversed $[Na^+]$ gradient. In normal $[Na^+]$ gradient the Q_{10} for τ is 2.9 (control) and 2.6 (*n*PG). In reversed $[Na^+]$ gradient the Q_{10} is 2.6 (control) and 2.7 (*n*PG). Therefore, while *n*PG reduces τ by about one-half, the temperature dependence of this parameter is not significantly changed.

Concentration Dependence

Fig. 2 illustrates an interesting dependence of sodium channel behavior on the concentration of *n*PG. Points represent experimental data, recorded in axons in reversed $[Na^+]$ gradient. On the left we plot the ratio of peak currents with and without *n*PG, and on the right the corresponding ratio of decay time constants. The abscissa shows the internal concentration of

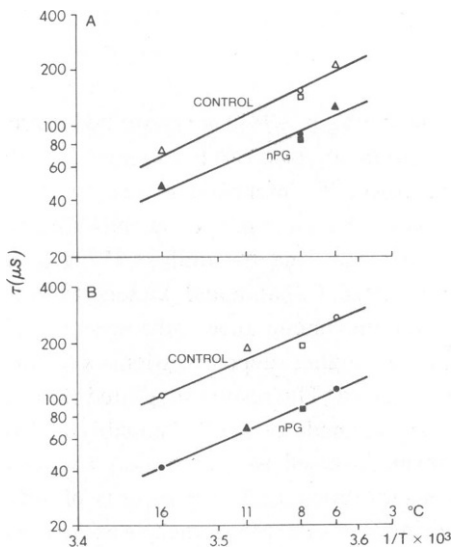

FIGURE 1 Temperature dependence of decay time constants. Arrhenius plots of τ vs. $1/T$ (K°). Temperature in °C is also indicated. *A*, axons in normal $[Na^+]$ gradient. *B*, axons in reversed $[Na^+]$ gradient. Symbols represent experimental results from six axons, with depolarizations to +90 mV. Internal [*n*PG] = 4.4 mM. Straight lines are least-square fits.

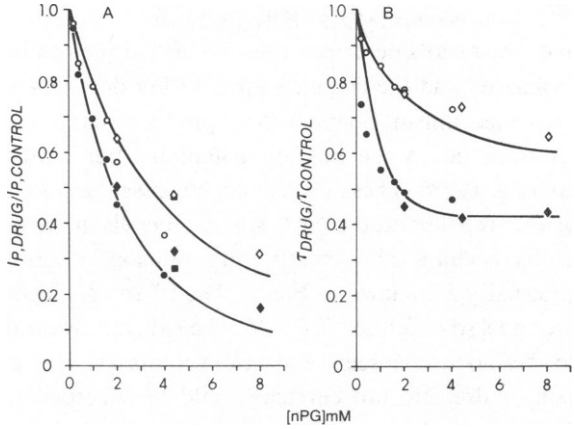

FIGURE 2 Concentration dependence of *n*PG on sodium channels. Axons in reversed [Na^+] gradient. Abscissa shows internal *n*PG concentration. *n*PG was washed out periodically to check control values. *A*, ratio of peak currents with and without drug. *B*, corresponding ratio of decay time constants. Points represent experimental data. Open symbols measured at 0 mV; filled symbols at +100 mV. Lines are calculated from a kinetic model discussed in the text. Rate constants used for these fits were taken from the points shown in Fig. 4 *B* at 0 mV and +100 mV.

*n*PG, which ranged from 0.2 to 8 mM. As different concentrations were tested, *n*PG was periodically washed out and control values remeasured. Most peak current ratios reflect averages of bracketing controls to correct for a slow run-down. Open symbols represent data at 0 mV and filled symbols at +100 mV. Peak currents decline rapidly with concentration, even at the highest levels tested. On the other hand, τ declines sharply at low [*n*PG], but reaches an asymptote above 4 mM. The lines represent fits of a kinetic model that is discussed below.

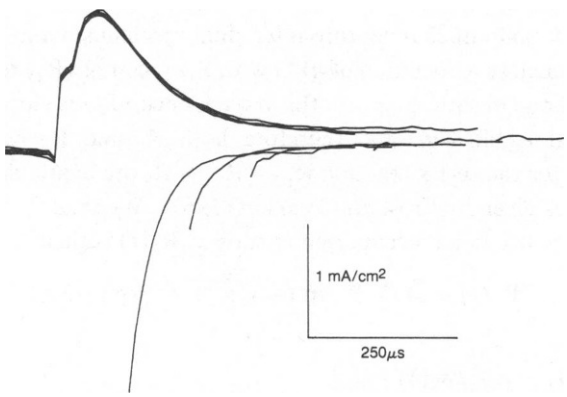

FIGURE 3 Sodium tail currents. Axon in normal [Na^+] gradient, with 4.4 mM *n*PG inside. Pulses to +90 mV were interrupted at times ranging from 0.1 to 0.7 ms and the potential brought to −70 mV. Traces are shown here superimposed. The fast capacitative transients (30 μs) are not seen on this scale. Temperature = 8°C.

Tail Currents

In one interpretation of the results described thus far, *n*PG is driven into Na^+ channels when the membrane is depolarized and the channels open. Other drugs have been found that seem to act through a similar mechanism. Some of these produce characteristic "hooks" in I_{Na} tail currents when V_m is returned to the holding potential after a depolarization (Yeh and Narahashi, 1977; Cahalan, 1978). These hooks may be present even if I_{Na} has been allowed to decay completely before repolarization, and kinetic models to explain drug action must account for these results. Sodium tail currents from an axon in normal [Na^+] gradient and with 4.4 mM *n*PG internally are shown in Fig. 3. The fiber was depolarized to +90 mV for varying periods before repolarization to −70 mV. The capacitative transients are too large to be seen in the figure. No hooks are seen, and tail currents are negligible after decay of I_{Na} during the depolarizing pulse. No tail currents could be recorded from axons in reversed [Na^+] gradients although several voltage protocols were attempted.

KINETIC MODEL

Rate Constants

A model for the interaction of *n*PG with sodium channels must account for the considerable variety of phenomena described thus far. In particular, it must explain the action of *n*PG on decay time constants, peak conductances, and tail currents, and the dependence of these effects on voltage, [Na^+] gradient, temperature, and *n*PG concentration. Further, as a test, we sought a model with a physical interpretation that would be compatible with suggestive evidence concerning gating mechanisms that has come from other laboratories. This will be detailed in the Discussion.

We consider that *n*PG may interact with a receptor in the Na^+ channel as outlined below:

$$n\text{PG} + \text{R}_1 \underset{k_{21}}{\overset{k_{12}}{\rightleftharpoons}} \text{R}_2 \underset{k_{32}}{\overset{k_{23}}{\rightleftharpoons}} \text{R}_3.$$

From the results of this and the previous paper (Lo and Shrager, 1981) we conclude that *n*PG must interact with the sodium channel through a dual mechanism and we therefore postulate two steps: the first is a close association of *n*PG with the receptor (R_1) to form the R_2 state. R_2 then undergoes a change in state to R_3. In this model, once *n*PG is closely associated with the receptor the channel is blocked, and therefore both R_2 and R_3 represent closed states. Analytical solutions for the series reaction $R_1 \rightleftharpoons R_2 \rightleftharpoons R_3$ are available and the result for R_2 and R_3 initially zero is given by Frost and Pearson (1961). We take $R_1 + R_2 + R_3 = 1$ so that each R_x represents the fractional occupation of state x. $R_1(t)$ is then:

$$\text{R}_1(t) = A + B\exp(-\lambda_2 t) + C\exp(-\lambda_3 t)$$

with $A = k_{21}k_{32}/\lambda_2\lambda_3$

$B = k_{12}(\lambda_2 - k_{23} - k_{32})/\lambda_2(\lambda_2 - \lambda_3)$

$C = k_{12}(k_{23} + k_{32} - \lambda_3)/\lambda_3(\lambda_2 - \lambda_3)$

where

$$\lambda_2 = (p + q)/2$$

$$\lambda_3 = (p - q)/2$$

and $p = k_{12} + k_{21} + k_{23} + k_{32}$

$$q = [p^2 - 4(k_{12}k_{23} + k_{21}k_{32} + k_{12}k_{32})]^{1/2}$$

We wished to see if this scheme could predict the form of Na^+ currents recorded in the presence of *n*PG. We generated theoretical currents by multiplying control records by $R_1(t)$, where R_1 is the fraction of Na^+ channels not blocked by the drug. In doing so, we include the assumption that the channel undergoes the normal inactivation process independent of *n*PG. The simplest interpretation of this model would be that the *n*PG receptor may be physically distinct from the inactivation machinery. The calculation is, however, also consistent with a common receptor for the drug and an inactivation gating component if the gate kinetics are not affected by *n*PG binding. This might be the case, for example, if normal inactivation involved several groups in addition to the one competing with *n*PG, and after binding of these groups, *n*PG is rapidly displaced. Only channels with open inactivation gates would be accessible to the drug, and $R_1(t)$ would then represent the fraction of these channels not blocked by *n*PG. This will be valid so long as the inactivation of some channels does not increase the effective drug concentration at open channels. For the range of channel densities reported for large fibers (Levinson and Meves, 1975; Jaimovich et al., 1976) and *n*PG concentrations of a few millimolar this would be expected.

In our calculations we also assume that the four rate constants for *n*PG action change abruptly with a change in membrane potential, i.e., the drug can interact with channels that are either resting or activated. Since *n*PG seems not to be use-dependent (Lo and Shrager, 1981) we have no evidence ruling out interaction with resting channels. We make no assumptions, however, with regard to a possible coupling of activation and inactivation in Na^+ channels. In multiplying control currents by R_1 we implicitly assume that inactivation proceeds as in the absence of drug, and require no further assumptions about its nature.

In our attempt to fit this model to the results we began with the dependence of peak currents and decay kinetics on *n*PG concentration. We found that the model was capable of accounting for the steep decline of peak currents and the asymptotic behavior of decay time constants. This calculation provided initial estimates for the rate constants at several voltages. The model was then refined by fitting complete sodium currents. The computer varied one rate constant at a time with increments made progressively smaller in succeeding calculations. Fits were monitored visually by superimposing records in *n*PG with model predictions, and were quantitated by calculating peak values and decay time constants for comparison with experimental results. We then chose the set of rate constants which, in our judgment, best satisfied all of the criteria discussed earlier. These are shown as functions of voltage in Fig. 4, for a temperature of 8°C. Fig. 4 *A* illustrates these parameters for an axon in normal [Na^+] gradient and Fig. 4 *B*, the corresponding data for reversed [Na^+] graident. The points represent rate constants used by the computer in calculating $R_1(t)$ and fitting actual records. The straight lines are least-square fits to these points. The fits are good, and all rate constants are simple exponential functions of voltage, at least within the range of V_m examined (-20 to $+120$ mV). The voltage dependence of the rate constants for the *n*PG + $R_1 \rightleftharpoons R_2$ reaction is shallow, and corresponds, at 8°C in normal [Na^+] gradient, to a site only 6–10% of the membrane field from the inner surface. The curves for k_{23} and k_{32} on the other hand suggest movement through 20–34% of the field during the $R_2 \rightleftharpoons R_3$ transition.

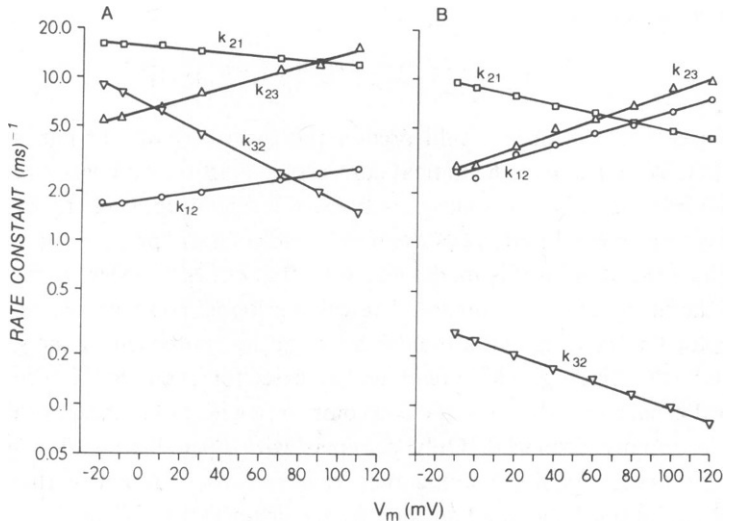

FIGURE 4 Rate constants used in the kinetic model, plotted vs. membrane potential. *A*, axons in normal [Na^+] gradient. *B*, axons in reversed [Na^+] gradient. Symbols represent best fits to experimental data. The straight lines are least-square fits. These rate constants have been used to generate the fitted curves in Figs. 2, 5, 6, 7, and 8. Units are ms^{-1} mM^{-1} for k_{12} and ms^{-1} for all other rate constants. Temperature = 8°C.

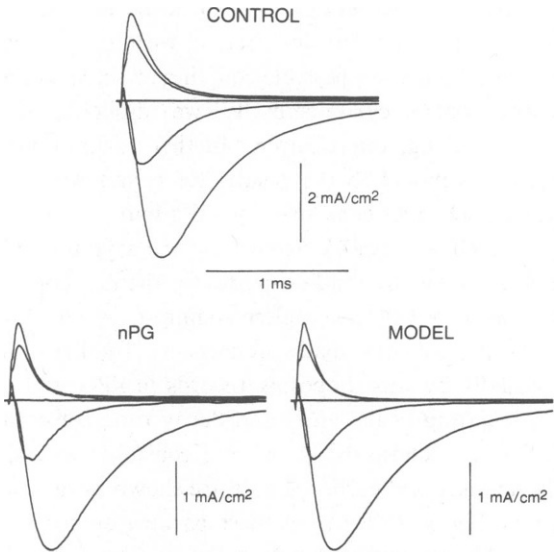

FIGURE 5 Fits of the model to sodium currents with *n*PG. Axon in normal [Na^+] gradient. The curves labeled "model" were generated by multiplying control currents by $R_i(t)$, calculated using the rate constants of Fig. 4 *A*. They are to be compared with the "*n*PG" curves, which are plotted to the same scale. The curves with drug have been multiplied by the ratio of driving forces in control/*n*PG to compensate for the small difference in reversal potentials, as noted in the previous paper (Lo and Shrager, 1981). Potassium currents were reduced by 2 mM 4-aminopyridine and eliminated by subtracting records in 100 nM tetrdotoxin. Depolarizations were from −70 mV to −10, +30, +90, and +110 mV. [*n*PG] = 4.4 mM internally. Temperature = 8°C.

Voltage Dependence

In Fig. 5 we show families of Na^+ currents from an axon in normal [Na^+] gradient. For clarity only four voltages are represented: −10, +30, +90, +110 mV. The top family shows control records. The lower left family gives results with 4.4 mM *n*PG added internally. Note different current scales. The lower right family represents a fit of our model to the *n*PG curves. Control records were multiplied by $R_1(t)$ using the rate constants given in Fig. 4 *A* for each V_m. The scale is the same as that for the *n*PG currents. The fit is satisfactory, predicting both the decrease in peak currents at all potentials, and the faster decay rate at high depolarizations. In Fig. 6 we illustrate corresponding data for an axon in reversed [Na^+] gradient. Test pulses were to 0, +40, +80, and +120 mV, and [*n*PG] was 4.0 mM. Rate constants used to calculate $R_1(t)$ at each V_m are given in Fig. 4 *B*. The model predicts a decay time constant that is somewhat too small at the highest depolarization. The peak currents are fit reasonably well. Note that the current scale is expanded and that there has been a fourfold decrease from control to *n*PG.

Detailed peak currents and decay time constants are given in Figs. 7 and 8 for normal and reversed [Na^+] gradients, respectively. The circles show experimental results with *n*PG (values without drug are not shown). The crosses give corresponding parameters derived from fits such as those shown in Figs. 5 and 6, but including more voltages. The lines are smooth curves joining the crosses and were drawn by eye. The model thus fits records in *n*PG satisfactorily, with the few exceptions noted above.

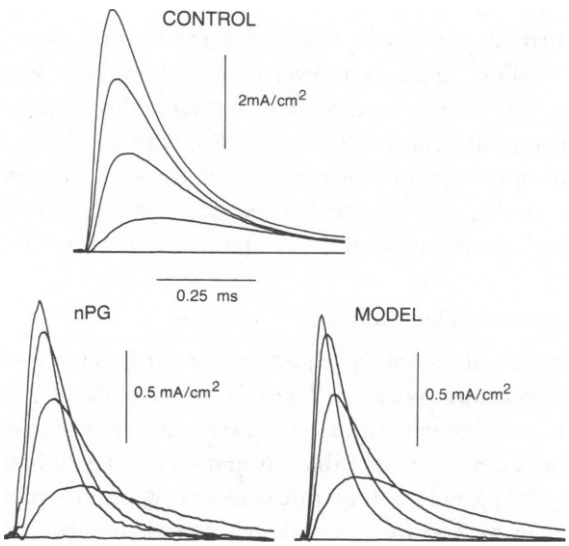

FIGURE 6 Fits of the model to sodium currents in the presence of *n*PG. Axon in reversed [Na^+] gradient. The curves labeled "model" have been generated by multiplying control currents by $R_1(t)$, calculated using the rate constants of Fig. 4 *B*. They should be compared with the "*n*PG" currents, plotted to the same scale. Note the large difference from the control scale. Holding potential = −50 mV. A prepulse to −110 mV for 50 ms and a 0.5 ms return to −50 mV preceded depolarizations to 0, 40, 80, and 120 mV. [*n*PG] = 4.0 mM internally. Solutions: Na2.3VH//Na213. Temperature = 8°C.

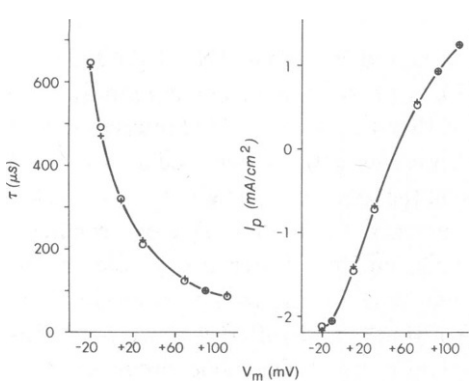

FIGURE 7

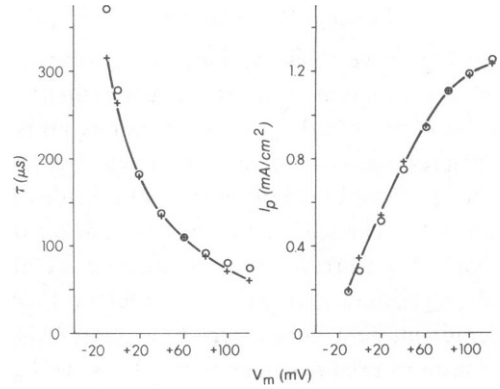

FIGURE 8

FIGURE 7 Fit of the model to decay time constants and peak currents. Axon in normal [Na^+] gradient. Crosses were calculated by first generating "model" curves as in Fig. 5 and then measuring τ and I_p from them. The lines were drawn by eye connecting the crosses to indicate trends. The circles represent experimental values, with [*n*PG] = 4.4 mM internally. Temperature = 8°C.

FIGURE 8 Fit of the model to decay time constants and peak currents. Axon in reversed [Na^+] gradient. Crosses were calculated by first generating "model" curves as in Fig. 6 and then measuring τ and I_p from them. The lines were drawn by eye connecting the crosses to indicate trends. The open circles represent experimental values, with [*n*PG] = 4.0 mM internally. Solutions: Na2.3VH//Na213. Temperature = 8°C.

Concentration Dependence

Variation of peak currents and decay times with the internal concentration of *n*PG was measured at 0 and +100 mV in axons in reversed [Na^+] gradient. Rate constants for our fit were taken from Fig. 4 *B* at the corresponding voltages. For calculation of $R_1(t)$, k_{12} was multiplied by the appropriate concentration of *n*PG, with the latter incremented in small steps. After generation of fitted clamp currents, I_{peak} and τ were measured from the fit and are plotted as the curves in Fig. 2. The model successfully predicts the steep decrease in peak currents with [*n*PG] and the corresponding asymptotic behavior of decay time constants.

Model Temperature Dependence

We have tested the model for its ability to account for variation of decay time constants and peak currents with temperature. We chose fibers for which data were available at both 6° and 16°C. Rate constants were chosen to fit the *n*PG curves at +90 mV and at 6°C. The Q_{10} for τ_h measured in control records is given in Table I A and Fig. 1 as 2.89 in normal [Na^+] gradient and 2.55 in reversed [Na^+] gradient. If all rate constants were multiplied by 2.89 for a fiber in normal Na^+ gradient (or by 2.55 for reversed [Na^+] gradient) then the model gave the time constant of I_{Na} decay at 16°C accurately, but predicted too strong a depression of peak currents. If, however, these high Q_{10} were used only for the second step of the reaction sequence (k_{23} and k_{32}) and a Q_{10} of 1.3, close to that of free diffusion, used for the first step (k_{12} and k_{21}) then the model satisfactorily predicted both I_p and τ. Results are summarized in Table I. Rate constants and Q_{10} used are given in part B of Table I. In part C we give control

TABLE IA
TEMPERATURE DEPENDENCE OF THE KINETIC MODEL: MEASURED CONTROL Q_{10}

[Na⁺] gradient	τ_h		Q_{10}
	6°C	16°C	
	ms	*ms*	
Normal	0.211	0.073	2.89
Reversed	0.270	0.106	2.55

TABLE IB
TEMPERATURE DEPENDENCE OF KINETIC MODEL: RATE CONSTANTS

Rate constant	Normal [Na⁺] gradient			Reversed [Na⁺] gradient		
	6°C	Q_{10} used	16°C	6°C	Q_{10} used	16°C
	ms^{-1}		ms^{-1}	ms^{-1}		ms^{-1}
$k_{12} \times$ [*n*PG]*	14.00	1.30	18.20	32.00	1.30	41.60
k_{21}	11.00	1.30	14.30	4.50	1.30	5.85
k_{23}	11.00	2.89	31.79	6.50	2.55	16.60
k_{32}	1.00	2.89	2.89	0.14	2.55	0.36

*[*n*PG] = 4.4 mM

TABLE IC
TEMPERATURE DEPENDENCE OF KINETIC MODEL: DECAY τ AND PEAK Na^+ CURRENTS

[Na⁺] gradient	Temp.	τ			I_P		
		Control	*n*PG	Model	control	*n*PG	Model
	°C	*ms*	*ms*	*ms*	mA/cm^2	mA/cm^2	mA/cm^2
Normal	6	0.211	0.127	0.126	1.36	0.55	0.54
	16	0.073	0.047	0.050	3.29	1.75	1.81
Reversed	6	0.270	0.113	0.114	11.15	1.81	1.81
	16	0.106	0.041	0.043	17.38	4.22	3.86

values of τ and I_P, measurements in *n*PG, and fits of the model. The "*n*PG" and "model" numbers at 16° (underlined pairs) are close in all cases, indicating adequacy of the fit.

Double-pulse Inactivation

In the previous paper (Lo and Shrager, 1981) we compared the kinetics of inactivation measured from I_{Na} decay (τ_h) with those measured from a double-pulse procedure (τ_c) (Goldman and Schauf, 1972). We found that for strong depolarizations *n*PG reduced τ_c along with τ_h in reversed [Na^+] gradient. In normal [Na^+] gradient, however, τ_c remained at control levels in *n*PG despite decreases in τ_h. This suggests that the drug is removed from the channel within 200–500 μs at -60 to -70 mV when the external [Na^+] is high, and that removal requires >1 ms when the external [Na^+] is low.

Applying our kinetic model to double-pulse experiments is difficult since it requires solutions from various specified initial conditions. We have attempted only rough calculations

to determine consistency. The reaction was first run "forward" for 100 μs at +90 mV. Rate constants at −70 mV were then estimated by extrapolating the curves in Fig. 4, and the degree of reversal to the R_I state was estimated after 200–1,000 μs. Despite a few approximations required in this last calculation, it was clear that this procedure could not account for the differences observed in the different [Na^+] gradients. Using the extrapolated rate constants the model predicts equivalence of τ_c and τ_h in both cases. The difficulty may lie in assuming that the simple exponential dependence on voltage found for the rate constants above −20 mV holds at more negative potentials. If, in particular, *n*PG acts only on open channels, as seems to be the case for drugs showing "use dependence" (Strichartz, 1973; Hille, 1977; Cahalan and Almers, 1979), then a sharp drop in k_{12}, and possible changes in other rate constants, would occur in the region of V_m corresponding to activation.

Na^+ Tail Currents

Because in our model we postulate that inactivation proceeds independently from *n*PG block, no tail currents would be expected if prepulse currents are allowed to decay to zero before repolarizing. This has been shown to be the case in Fig. 3. If repolarization is effected earlier, we can estimate the rate at which *n*PG would leave open channels by extrapolating the rate constants of Fig. 4 *A* to −70 mV. In this case the extrapolation may be valid since we are interested in events at very short times after the change in V_m. At this potential k_{21} and k_{32} would each be about 20 ms^{-1} and k_{12} and k_{23} would be much smaller. Thus, *n*PG would be expected to leave with a time constant of the order of 50 μs. This will overlap the fast capacitative transient, thus masking any "hooks." The model predications are therefore consistent with the records in Fig. 3.

DISCUSSION

In the previous paper (Lo and Shrager, 1981) it was shown that the speeding of I_{Na} decay kinetics by *n*PG is insufficient to explain the observed decrease in peak Na^+ conductance, suggesting that *n*PG acts in at least two ways. This conclusion is strengthened by the results with varying drug concentrations. The decay time constant approached an asymptote as the [*n*PG] rose above 4 mM, while peak Na^+ current continued to decline (Fig. 2). We first considered, therefore, a model involving two sites. As has been discussed (Lo and Shrager, 1981), the decrease in both τ and I_P is sensitive to V_m and [Na^+] gradient, suggesting that both sites must be within the sodium channel. At one site, *n*PG would bind rapidly and block the channel. At the second site, *n*PG may either alter the rate of closing of the inactivation gate (β_h) or enter the channel with a rate constant comparable to β_h and block. In the former case, the increase in β_h could not result simply from electrostatic forces, since the decrease in decay time constant was not represented by a simple shift along the voltage axis (Lo and Shrager, 1981). This site must therefore involve a close association with the *h*-gate, and since our evidence suggests a locus inside the sodium channel, we consider it unlikely that binding of *n*PG will not in itself result in block. Furthermore, results of the double-pulse experiments in normal [Na^+] gradient would require that α_h (the rate of opening of the *h*-gate) be speeded by *n*PG at least 50-fold at −70 mV, which may be unreasonable. Consideration of a two-site model thus leads to the conclusion that both sites must involve block, and that the sites are characterized by quite different kinetics and dissociation constants. This might well allow

sufficient freedom to achieve a fit to the data, but it also makes large demands on the channel structure. We chose, therefore, to try a simpler system.

We sought a model that would involve only one site within the sodium channel, and would allow a test of the evidence from other laboratories that arginine might be closely associated with inactivation (see Introduction). The model that has been adopted has two reaction steps, and the sequence suggests that the first step invovles a binding, or at least a close association of *n*PG with a receptor. The second reaction would then represent a change in state of the bound complex. Our fit to the temperature dependence of *n*PG action supports this view. The Q_{10} fitted to the first step is 1.3, while that for the second step is 2.6 to 2.9. Thus, the reaction: $n\text{PG} + R_1 \rightleftharpoons R_2$ may reflect diffusion of the drug to the receptor site, and association with it. Thermodynamic calculations provide supportive evidence. From the rate constants, k_{12} and k_{21} (6°C, normal $[Na^+]$ gradient) and their Q_{10} we have for the "association" step: $\Delta G° = -3.2$ kcal/mol, $\Delta H° = 0$ and $\Delta S° = +11.2$ e.u. The corresponding values for reversed Na^+ gradient are -4.1, 0, and $+14.6$, respectively. These numbers are very similar to those for the binding of small aliphatic anions to proteins: e.g., for $CH_3 - (CH_2)_6 - COO^-$ and bovine serum albumin, $\Delta G°$, $\Delta H°$, and $\Delta S°$ are -3.0, 0, and $+10.9$, respectively (calculated from Boyer et al., 1947). The increase in entropy on binding may result in part from altered hydration order due to a salt linkage and in part from a transfer of the hydrocarbon chain from water to a more apolar environment in the membrane (Kauzmann, 1959). The second step ($R_2 \rightleftharpoons R_3$) may then represent a conformational change in the receptor or some further process in binding. The high Q_{10} for this step corresponds to a high activation energy (15 kcal/mol, normal $[Na^+]$ gradient; 17 kcal/mol, reversed $[Na^+]$ gradient).

The asymptotic behavior of τ with *n*PG (Fig. 2) is a result of the relative rates of the two reactions. The first, or association, step occurs rapidly, with a rate proportional to drug concentration. The R_2 state reaches a maximum occupancy within about 50 μs and therefore has a large influence on peak Na^+ conductance. Further association must await filling of the R_3 state, which occurs at a slower rate. Increasing [*n*PG] above 4 mM fills R_2 faster and to a higher maximum level, resulting in a further decline of peak current. However, after about 100 μs the $R_2 \rightarrow R_3$ step becomes rate limiting, and maintains the rate of I_{Na} decay.

The dependence of *n*PG action on $[Na^+]$ gradient is explained in the following way. There is evidence that at least one binding site for Na^+ ions exists within the sodium channel, and that the energy well is located near the external opening of the channel (Strichartz, 1973; Hille, 1975). The inactivation mechanism, and hence also the receptor for *n*PG in our model, is thought to be close to the internal surface (Armstrong et al., 1973; Shrager and Starkus, 1979). In the fit of our model the rate constant most sensitive to the $[Na^+]$ gradient is k_{32}. It is higher by a factor of more than 10 in normal $[Na^+]$ gradient (Fig. 4). A sodium ion bound at a site external to that of *n*PG might exert sufficient electrostatic force to increase k_{32} significantly. The difference in activation energy for the $R_2 \leftarrow R_3$ transition between the two $[Na^+]$ gradients is 1.6 kcal/mol at $+100$ mV. In the above physical interpretation this would imply that the drug-receptor complex is closer to the bound Na^+ ion in the R_3 state than in the R_2 state. In this hypothesis the external Na^+ ions have access to their binding site when *n*PG is present, but internal Na^+ ions can be prevented from traversing the inner portion of the channel and reaching this site when the drug is within the channel. Thus, high external $[Na^+]$ reduces the effectiveness of *n*PG, compared with high internal $[Na^+]$. Effects of the $[Na^+]$

gradient on other rate constants are much weaker. The lower k_{12} and higher k_{21} in normal $[Na^+]$ gradient are also consistent with a raised potential at a site external to the *n*PG receptor when a sodium ion is bound.

Perhaps the weakest aspect of our kinetic scheme is the suggestion that inactivation proceeds at the same rate regardless of the drug-receptor state. This is probably physically unreasonable, but was included to avoid introducing further degrees of freedom for the fit. It is also possible that the R_3 state represents in itself the displacement of *n*PG by the normal inactivation mechanism, or perhaps the gate "closing behind" the drug. Also, as mentioned earlier, the model assumes no delay for *n*PG action after a depolarization. We had no direct evidence that the drug required prior channel activation. Goldman and Schauf (1972) have found a coupling of inactivation to activation in *Myxicola* fibers. The demonstration of gating charge immobilization by Armstrong and Bezanilla (1977) is evidence that normal inactivation follows activation. However, recent studies in squid (Gillespie and Meves, 1980) and in crayfish (Bean, 1979) axons suggest that strict coupling of these processes is not likely, although some activation steps may be required for inactivation of a channel.

The model presented is the simplest system that we were able to develop that would explain the results of this and the previous paper. There is ample precedent for a two-step reaction in ligand-receptor interactions. An obvious example relevant to membrane channels is the binding of acetylcholine to muscle end-plate receptors (Magleby and Stevens, 1972). It is interesting in this regard that Yeh and Armstrong (1978) found that pancuronium appeared to interfere with an inactivation-resistant portion of "off" gating current. These authors postulate that this component of gating current may be associated with a transition that holds the channel closed during recovery from inactivation.

Our model satisfactorily explains the influence of *n*PG on peak conductance and on decay kinetics at a variety of voltages, drug concentrations, Na^+ concentrations, and temperatures. It does so with rate constants that are simple exponential functions of membrane potential. In developing a simplified model that allowed so thorough a description of the receptor, we necessarily sacrificed information about possible identity of this site with normal channel components. As discussed in introducing the scheme, our model cannot distinguish between a site distinct from inactivation and one that is common to the inactivation system, but obeys our assumption of independent kinetics. Work from other laboratories provides information useful for further resolution of these possibilities. From studies of gating charge immobilization, Armstrong and Bezanilla (1977) developed a model for sodium channel inactivation. In response to a depolarization, charge movement during activation renders the internal channel surface more negative. A membrane component with positive charge is then attracted to this site, occluding the channel. These authors found no gating current component associated with inactivation and the occluding step was therefore considered to be voltage independent. In our model, the voltage dependence of k_{12} and k_{21} suggests that the receptor for *n*PG is only a small percentage of the field from the inner surface (see Results). Charge that moved through just 10% of the field and had the slow kinetics of inactivation would be difficult to detect as gating current. Further, while *n*PG and other cationic blockers may have to move some distance into the channel, an endogenous inactivating component may move primarily within the plane of the membrane. Thus, *n*PG, and possibly other organic ions (Rojas and Rudy, 1976; Yeh and Narahashi, 1977; Hille, 1977; Cahalan and Almers, 1979) may interact at a site common to normal inactivation. Unlike *n*PG, the other drugs that have been found to block sodium

channels are generally large, and have no apparent relationship with normally occurring membrane chemistry. In showing that the side chain of arginine may also result in "inactivation" we provide a possible biochemical candidate for this component of the channel.

We thank Mrs. Wendy Keck for excellent secretarial assistance.

This work has been supported by the National Institutes of Health through research grant 5-RO1-NS10500 and Research Career Development Award 1-KO4-NS00133 (to Dr. Shrager).

Received for publication 30 July 1980 and in revised form 9 February 1981.

REFERENCES

Armstrong, C. M., and F. Bezanilla. 1977. Inactivation of the sodium channel. II. Gating current experiments. *J. Gen. Physiol.* 70:567–590.

Armstrong, C. M., F. Bezanilla, and E. Rojas. 1973. Destruction of sodium conductance inactivation in squid axons perfused with pronase. *J. Gen. Physiol.* 62:375–391.

Bean, B. P. 1979. Modification of sodium and potassium channel kinetics by diethyl ether and studies on sodium channel inactivation in the crayfish giant axon membrane. Thesis. University Microfilms, Ann Arbor, Mich.

Boyer, P. D., G. A. Ballon, and J. M. Luck. 1947. The combination of fatty acids and related compounds with serum albumin. III. The nature and extent of the combination. *J. Biol. Chem.* 167:407–424.

Cahalan, M. D. 1978. Local anesthetic block of sodium channels in normal and pronase-treated squid giant axons. *Biophys. J.* 23:285–311.

Cahalan, M. D., and W. Almers. 1979*a*. Interaction between quarternary lidocaine, the sodium channel gates, and tetrodotoxin. *Biophys. J.* 27:39–56.

Cahalan, M. D., and W. Almers. 1979*b*. Block of sodium conductance and gating current in squid giant axons poisoned with quaternary strychnine. *Biophys. J.* 27:57–74.

Eaton, D. C., M. S. Brodwick, G. S. Oxford, and B. Rudy. 1978. Arginine-specific reagents remove sodium channel inactivation. *Nature (Lond.).* 271:473–475.

Frost, A. A., and R. G. Pearson. 1961. Complex reactions. *In* Kinetics and Mechanism. 2nd edition. John Wiley and Sons, Inc., New York. p. 173–177.

Gillespie, J. I., and H. Meves. 1980. The time course of sodium inactivation in squid giant axons. *J. Physiol. (Lond.).* 299:289–307.

Goldman, L., and C. L. Schauf. 1972. Inactivation of the sodium current in *Myxicola* giant axons. Evidence for coupling to the activation process. *J. Gen. Physiol.* 59:659–675.

Hille, B. 1975. Ionic selectivity, saturation, and block in sodium channels. A four barrier model. *J. Gen. Physiol.* 66:535–560.

Hille, B. 1977. Local anesthetics: hydrophilic and hydrophobic pathways for the drug-receptor reaction. *J. Gen. Physiol.* 69:497–515.

Jaimovich, E., R. A. Venosa, P. Shrager, and P. Horowicz. 1976. Density and distribution of tetrodotoxin receptors in normal and detubulated frog sartorius muscle. *J. Gen. Physiol.* 67:399–416.

Kauzmann, W. 1959. Some factors in the interpretation of protein denaturation. *Adv. Protein Chem.* 14:1–63.

Levinson, S. R., and H. Meves. 1975. The binding of tritiated tetrodotoxin to squid giant axons. *Philos. Trans. R. Soc. Lond. B. Biol. Sci.* 270:349–352.

Lo, M-V. C., and P. Shrager. 1981. Block and inactivation of sodium channels in nerve by amino acid derivatives. I. Dependence on voltage and sodium concentration. *Biophys. J.* 35:31–43.

Magleby, K. L., and C. F. Stevens. 1972. A quantitative description of end-plate currents. *J. Physiol. (Lond.).* 223:173–197.

Rojas, E., and B. Rudy. 1976. Destruction of the sodium conductance inactivation by a specific protease in perfused nerve fibers from *Loligo*. *J. Physiol. (Lond.).* 262:501–531.

Shrager, P., and J. G. Starkus. 1979. Block of sodium inactivation in nerve by polyphenols: ion accumulation in the Schwann cell space. *Biophys. J.* 25:306*a*.

Strichartz, G. R. 1973. The inhibition of sodium currents in myelinated nerve by quaternary derivatives of lidocaine. *J. Gen. Physiol.* 62:37–57.

Yeh, J. Z., and C. M. Armstrong. 1978. Immobilization of gating charge by a substance that simulates inactivation. *Nature (Lond.)* 273:387–389.

Yeh, J. Z., and T. Narahashi. 1977. Kinetic analysis of pancuronium interaction with sodium channels in squid axon membranes. *J. Gen. Physiol.* 69:293–323.